

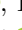
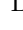













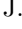
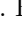

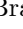
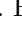




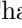
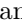
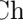

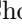
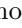



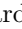

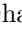












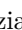






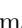


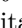
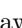

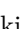
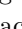


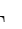








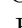





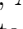




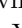

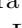
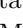
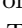
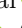


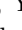
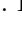
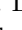
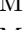
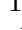


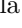



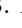
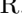
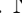










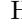
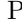


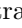


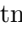


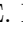
















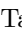
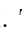

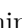
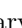

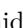

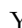
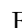

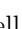
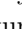
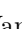
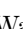

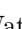


Search for Baryon-Number-Violating Processes in B^- Decays to the $\Xi_c^0 \bar{\Lambda}_c^-$ Final State

T. Gu , V. Savinov , I. Adachi , H. Aihara , D. M. Asner , H. Atmacan , T. Aushev , R. Ayad ,
Sw. Banerjee , K. Belous , J. Bennett , M. Bessner , V. Bhardwaj , B. Bhuyan , D. Biswas , A. Bobrov ,
D. Bodrov , J. Borah , A. Bozek , M. Bračko , P. Branchini , T. E. Browder , A. Budano , M. Campajola ,
D. Červenkov , M.-C. Chang , P. Chang , B. G. Cheon , K. Chilikin , K. Cho , S.-K. Choi , Y. Choi ,
S. Choudhury , S. Das , G. De Nardo , G. De Pietro , R. Dhamija , F. Di Capua , J. Dingfelder ,
Z. Doležal , T. V. Dong , S. Dubey , P. Ecker , T. Ferber , D. Ferlewicz , B. G. Fulsom , V. Gaur ,
A. Giri , P. Goldenzweig , E. Graziani , Y. Guan , K. Gudkova , C. Hadjivasiliou , K. Hayasaka ,
H. Hayashii , M. T. Hedges , D. Herrmann , W.-S. Hou , C.-L. Hsu , N. Ipsita , A. Ishikawa , R. Itoh ,
M. Iwasaki , W. W. Jacobs , S. Jia , Y. Jin , K. K. Joo , T. Kawasaki , C. Kiesling , C. H. Kim ,
D. Y. Kim , K.-H. Kim , Y. J. Kim , P. Kodyš , A. Korobov , S. Korpar , E. Kovalenko , P. Križan ,
P. Krokovny , T. Kuhr , K. Kumara , T. Kumita , Y.-J. Kwon , Y.-T. Lai , S. C. Lee , D. Levit ,
L. K. Li , Y. B. Li , L. Li Gioi , D. Liventsev , M. Masuda , T. Matsuda , S. K. Maurya , F. Meier ,
M. Merola , F. Metzner , K. Miyabayashi , R. Mizuk , G. B. Mohanty , R. Mussa , I. Nakamura ,
M. Nakao , Z. Natkaniec , A. Natchii , L. Nayak , M. Nayak , M. Niiyama , S. Nishida , S. Ogawa ,
G. Pakhlova , S. Pardi , H. Park , J. Park , S.-H. Park , A. Passeri , S. Patra , S. Paul , T. K. Pedlar ,
R. Pestotnik , L. E. Piilonen , T. Podobnik , E. Prencipe , M. T. Prim , M. Röhrken , G. Russo ,
S. Sandilya , L. Santelj , G. Schnell , C. Schwanda , Y. Seino , K. Senyo , M. E. Sevier , W. Shan ,
C. Sharma , J.-G. Shiu , E. Solovieva , M. Starič , M. Takizawa , U. Tamponi , K. Tanida ,
F. Tenchini , R. Tiwary , K. Trabelsi , M. Uchida , Y. Unno , S. Uno , Y. Usov , S. E. Vahsen ,
K. E. Varvell , A. Vinokurova , E. Wang , M.-Z. Wang , X. L. Wang , S. Watanuki , E. Won , X. Xu ,
B. D. Yabsley , W. Yan , S. B. Yang , L. Yuan , Z. P. Zhang , V. Zhilich , and V. Zhukova 

(The Belle Collaboration)

We report the results of the first search for B^- decays to the $\Xi_c^0 \bar{\Lambda}_c^-$ final state using 711 fb⁻¹ of data collected at the $\Upsilon(4S)$ resonance with the Belle detector at the KEKB asymmetric-energy e^+e^- collider. The results are interpreted in terms of both direct baryon-number-violating B^- decay and $\Xi_c^0 - \bar{\Xi}_c^0$ oscillations which follow the Standard Model decay $B^- \rightarrow \Xi_c^0 \bar{\Lambda}_c^-$. We observe no evidence for baryon number violation and set the 95% confidence-level upper limits on the ratio of baryon-number-violating and Standard Model branching fractions $\mathcal{B}(B^- \rightarrow \Xi_c^0 \bar{\Lambda}_c^-)/\mathcal{B}(B^- \rightarrow \Xi_c^0 \bar{\Lambda}_c^-)$ to be $< 2.7\%$ and on the $\Xi_c^0 - \bar{\Xi}_c^0$ oscillation angular frequency ω to be $< 0.76 \text{ ps}^{-1}$ (equivalent to $\tau_{\text{mix}} > 1.3 \text{ ps}$).

PACS numbers: 11.30.Fs, 13.30.-a, 13.20.He

Understanding the origin of the matter-antimatter asymmetry of the universe is one of the greatest challenges in particle physics. Three conditions necessary for baryogenesis, a hypothesized physical process necessary for generating such asymmetry in the early universe are (1) baryon number violation (BNV), (2) C and CP violation, and (3) departure from thermal/chemical equilibrium [1]. Of these three Sakharov conditions, experimental evidence for CP violation has been observed and departure from thermal equilibrium could, in certain extensions of the Standard Model (SM), be satisfied through the expansion of the universe. No experimental evidence for BNV has been obtained so far. An observation of BNV would provide the missing piece of the puzzle of baryogenesis and would be a pathway to understand

the origin of the baryon asymmetry of the universe.

A variety of processes can be used to search for BNV, *e.g.*, proton decay [2], which was originally proposed as a way to probe physics at the energy scale of grand unification, and direct BNV decays of the τ lepton [3, 4] and B mesons [5], whose rates are usually extremely suppressed [6]. Most of such BNV processes would be mediated by transitions which violate two discrete quantum numbers, baryon number B and lepton number L , but conserve the difference $\Delta(B - L)$ between them. Both B and L numbers are, from the perspective of the SM, accidental, *i.e.*, not protected by gauge symmetries, and could be violated non-perturbatively at high temperatures in the early universe [7]. Existing experimental data strongly constrain new physics in such $\Delta(B - L) = 0$

processes. The exploration of the BNV landscape has recently been expanded to the domain of $\Delta(B-L) = 2$ processes via baryon-antibaryon oscillations. The flagship effort, motivated by the discovery of neutrino oscillations which require $\Delta(B-L) = 2$ interactions in the seesaw mechanism [8–10], is in the area of neutron-antineutron oscillations [11]. Recently, the BES III experiment extended the search for $\Delta(B-L) = 2$ processes to include the s quark via $\Lambda^0 - \bar{\Lambda}^0$ oscillations and obtained a stringent limit [12] on the time constant of such oscillations to be $\tau_{\text{mix}} > 1.7 \times 10^{-7}$ s at the 90% confidence level (C.L.). The LHCb experiment performed a similar search [13] for $\Xi_b^0 - \bar{\Xi}_b^0$ oscillations in the bottom sector and set the 95% C.L. upper limit on the oscillation rate to be $\omega < 0.08 \text{ ps}^{-1}$ (equivalent to $\tau_{\text{mix}} = 1/\omega > 13 \text{ ps}$). In this Letter we expand the study of baryon-antibaryon oscillations to include the charm sector and report the results of the first search for BNV processes in B^- decays to the $\Xi_c^0 \bar{\Lambda}_c^-$ final state. The unique feature of the analysis presented here is our ability to probe $\Delta(B-L) = 2$ processes which can proceed through several pathways. Such BNV transitions could be due to the direct BNV decay of B^- , which, similarly to BNV in τ lepton decays, is likely to be extremely suppressed. Also, they could be the result of the SM decay of B^- followed by two possible scenarios associated with Ξ_c^0 : the direct BNV process and $\Xi_c^0 - \bar{\Xi}_c^0$ oscillations, which were recently proposed [14] as a possible new mechanism for baryogenesis. The proposed model introduces CP -violating oscillations of neutral, heavy-flavor baryons into antibaryons at rates which are within a few orders of magnitude of their lifetimes. The model introduces four new particles: three light Majorana fermions and a colored scalar. The lightest of these fermions is typically long lived (on collider time scales) and may be produced in decays of bottom and possibly charmed baryons. Alternatively, such baryons could be created in the early universe via out-of-equilibrium decays of this Majorana fermion after hadronization but before nucleosynthesis. Therefore, this novel approach to baryogenesis also fulfills the out-of-equilibrium Sakharov condition. The discussed model could be easily embedded in an R -parity-violating supersymmetric theory [15], providing important connections to solving the puzzle of dark matter and the unification of fundamental forces.

The connection between the two main BNV hypotheses considered in this Letter can be further clarified as follows. Since charmed baryons have a relatively short lifetime (e.g., the Ξ_c^0 lifetime is 0.152 ps [16]), we are not able to resolve their decay vertices with the Belle detector [17, 18]. Therefore, from the analysis perspective, the SM decay $B^- \rightarrow \Xi_c^0 \bar{\Lambda}_c^-$ followed by the oscillation of Ξ_c^0 into $\bar{\Xi}_c^0$ (or direct BNV decay of Ξ_c^0) is indistinguishable from the direct BNV decay $B^- \rightarrow \Xi_c^0 \bar{\Lambda}_c^-$.

We measure the ratio between B^- decay rates for the $\Xi_c^0 \bar{\Lambda}_c^-$ and $\bar{\Xi}_c^0 \bar{\Lambda}_c^-$ final states and interpret this result as

the ratio between branching fractions for direct BNV and SM decays. To address the charmed baryon-antibaryon oscillation hypothesis, assuming that the BNV decay of B^- is actually the previously observed [19] SM decay $B^- \rightarrow \Xi_c^0 \bar{\Lambda}_c^-$ followed by the non-SM $\Xi_c^0 - \bar{\Xi}_c^0$ oscillations, we measure their frequency. In our study, the final states $\Xi_c^0 \bar{\Lambda}_c^-$ and $\bar{\Xi}_c^0 \bar{\Lambda}_c^-$ are referred to as the SM and BNV modes, respectively. Charge conjugate modes are included throughout this Letter.

The Ξ_c^0 and $\bar{\Xi}_c^0$ baryons are produced as flavor eigenstates, and then evolve and decay as superpositions of eigenstates of the Hamiltonian. The time evolution depends on the mixing parameters $x = (M_1 - M_2)/\Gamma$ and $y = (\Gamma_1 - \Gamma_2)/2\Gamma$, where $M_{1,2}$ and $\Gamma_{1,2}$ are the masses and widths of the eigenstates and $\Gamma = (\Gamma_1 + \Gamma_2)/2$. Assuming no CP violation and small mixing parameters, the time evolution of the event rate ratio between BNV and SM decays of a Ξ_c^0 state is described by the standard mixing formalism [20] as

$$r(t) = \left(R_D + \sqrt{R_D} y' \Gamma t + \frac{x'^2 + y'^2}{4} \Gamma^2 t^2 \right) e^{-\Gamma t}, \quad (1)$$

where R_D is the ratio between branching fractions of Ξ_c^0 for direct BNV and SM modes, $x' = x \cos \delta + y \sin \delta$, $y' = -x \sin \delta + y \cos \delta$, and δ is the strong phase difference between direct BNV and SM decays (with mixing). The time-integrated ratio between decay rates for the BNV and SM modes is described by

$$R = R_D + \sqrt{R_D} y' + \frac{x'^2 + y'^2}{2}. \quad (2)$$

Assuming the $\Xi_c^0 - \bar{\Xi}_c^0$ oscillation hypothesis only and no direct BNV decay of Ξ_c^0 (i.e., $R_D = 0$), the time-integrated ratio of the decay rates for the BNV and SM modes is given by

$$R = 2 \left[\left(\frac{\Delta M}{2} \right)^2 + \left(\frac{\Delta \Gamma}{4} \right)^2 \right] \tau^2 = 2\omega^2 \tau^2, \quad (3)$$

where $\Delta M = M_1 - M_2$, $\Delta \Gamma = \Gamma_1 - \Gamma_2$, ω is the angular frequency of $\Xi_c^0 - \bar{\Xi}_c^0$ oscillations and τ is the lifetime of Ξ_c^0 .

In the presence of a magnetic field, the non-zero magnetic moment of baryons results in an energy splitting $\Delta E = 2\mu B$ of the baryon and anti-baryon states. This energy splitting leads to suppression of oscillations. The criterion for neglecting the effect is $|\Delta E|t/2 \ll 1$, where t is the time of propagation of the baryon [11]. We assume the magnetic moment of Ξ_c^0 to be comparable to the nuclear magneton. The magnetic field of the Belle solenoid is 1.5 T and the Lorentz boost factor γ is 1.09. For the Ξ_c^0 lifetime τ of 1.519×10^{-13} s [16], $|\Delta E|t/2 = \mu\gamma B\tau \lesssim 10^{-5} \ll 1$. Therefore, the effect of the magnetic field can be safely ignored.

This analysis is based on the full data sample of 711 fb^{-1} collected at the $\Upsilon(4S)$ resonance with the Belle detector at the KEKB asymmetric-energy e^+e^- collider [21]. The Belle detector is a large-solid-angle magnetic spectrometer that consists of a silicon vertex detector (SVD), a 50-layer central drift chamber (CDC), an array of aerogel threshold Cherenkov counters (ACC), a barrel-like arrangement of time-of-flight scintillation counters (TOF), and an electromagnetic calorimeter comprised of CsI(Tl) crystals (ECL) located inside a super-conducting solenoid coil that provides the aforementioned 1.5 T magnetic field. An iron flux-return located outside of the coil is instrumented to detect K_L^0 mesons and to identify muons (KLM). The detector is described in detail elsewhere [17, 18].

Several signal Monte Carlo (MC) samples are generated to develop the signal selection criteria and estimate the reconstruction efficiencies. The MC generators EVTGEN [22], PHOTOS [23] and PYTHIA [24] are used to simulate hadronic decay processes, final state radiation and hadronization, respectively. The GEANT3 [25] toolkit is used to model the detector response. To study backgrounds we use an MC sample of $\Upsilon(4S) \rightarrow B\bar{B}$ and $e^+e^- \rightarrow q\bar{q}$ hadronic continuum events with $q = u, d, s, c$ at $\sqrt{s} = 10.58 \text{ GeV}$ corresponding to six times the integrated luminosity of the Belle data. Both background sources contribute to the events remaining after applying all selection criteria.

In our analysis, the Ξ_c^0 is reconstructed in three decay channels ($\Xi^-\pi^+$, $\Lambda^0 K^-\pi^+$ and $pK^-K^-\pi^+$), and the $\bar{\Lambda}_c^-$ is reconstructed in two decay channels ($\bar{p}K_S^0$ and $\bar{p}K^+\pi^-$). Thus a total of six decay channels of B^- mesons are analyzed. The Ξ^- , Λ^0 and K_S^0 candidates are reconstructed via $\Xi^- \rightarrow \Lambda^0\pi^-$, $\Lambda^0 \rightarrow p\pi^-$ and $K_S^0 \rightarrow \pi^+\pi^-$ decays, respectively.

Final state charged particles are required to have transverse momenta (in the plane perpendicular to the direction of the e^+ beam) above $50 \text{ MeV}/c$. To identify them we use information from the CDC, TOF, and ACC and prepare particle identification (PID) likelihoods [26] L_i for particle species $i = K, \pi, p$. Distinct likelihoods that also include ECL information are used to distinguish electron (e) and non-electron (h) hypotheses. We use the ratios of the PID likelihoods $R_{i/j} = L_i/(L_i + L_j)$ to select signal event candidates. Pions, kaons and protons are identified by requiring $R_{\pi/K} > 0.6$ and $R_{e/h} < 0.95$, $R_{\pi/K} < 0.6$ and $R_{e/h} < 0.95$, and $R_{p/K} > 0.6$ and $R_{p/\pi} > 0.6$, respectively. No such requirements are applied to the particles from K_S^0 and Λ^0 decays. The PID efficiency depends on the particle species and kinematics and varies between 92% and 98%. PID misidentification rate for hadrons is between 4% and 6% per particle.

K_S^0 and Λ^0 candidates are reconstructed in a multivariate analysis using a neural network technique [27, 28], and a kinematic fit to their decay vertices is performed to improve the mass resolution. The reconstructed masses

of the Λ^0 and K_S^0 candidates are required to be within $10 \text{ MeV}/c^2$ ($\approx \pm 5\sigma$) and $30 \text{ MeV}/c^2$ ($\approx \pm 10\sigma$) of the nominal Λ^0 and K_S^0 masses [16]. These requirements reject around 20% of background events and are at least 98%-efficient for signal events.

For each of the intermediate particle candidates ($K_S^0, \Lambda^0, \Xi^-, \Xi_c^0, \bar{\Lambda}_c^-$), the tracks reconstructed for its daughter particles are refit to a common vertex and their invariant mass is constrained to the nominal value. The momenta and decay vertices obtained from such constraints are then used in the parent particle reconstruction. The fit quality $\chi^2/n.d.f.$ is required to be smaller than 100 for each individual fit, where $n.d.f.$ is the number of degrees of freedom. This mass-vertex χ^2 -based requirement suppresses the background by a factor of 3. We apply the invariant mass requirements $|M_{\Xi_c^0} - m_{\Xi_c^0}| < 20 \text{ MeV}/c^2$, $|M_{\bar{\Lambda}_c^-} - m_{\bar{\Lambda}_c^-}| < 10 \text{ MeV}/c^2$ and $|M_{\Xi^-} - m_{\Xi^-}| < 10 \text{ MeV}/c^2$ ($\approx 3\sigma$ for each), where $M_{\Xi_c^0}$, $M_{\bar{\Lambda}_c^-}$ and M_{Ξ^-} are the reconstructed masses of Ξ_c^0 , $\bar{\Lambda}_c^-$ and Ξ^- candidates, and $m_{\Xi_c^0}$, $m_{\bar{\Lambda}_c^-}$ and m_{Ξ^-} are their nominal masses [16], respectively. The requirements applied to the reconstructed invariant masses after kinematic fitting remove 90% of the remaining background.

B^- candidates are identified using the beam-energy constrained mass $M_{bc} = \sqrt{(E_{\text{beam}})^2 - |\vec{p}_B|^2}$ and the energy difference $\Delta E = E_B - E_{\text{beam}}$, where E_{beam} is the beam energy, \vec{p}_B and E_B are the reconstructed momentum and energy of the B^- candidate, calculated in the e^+e^- center-of-mass frame. We require $M_{bc} > 5.20 \text{ GeV}/c^2$ and $|\Delta E| < 0.25 \text{ GeV}$; the efficiency of this selection exceeds 99%. The signal region is defined as $M_{bc} > 5.27 \text{ GeV}/c^2$ and $|\Delta E| < 0.02 \text{ GeV}$. The region $M_{bc} > 5.26 \text{ GeV}/c^2$ in the BNV analysis of data is blinded until the final fit to extract the branching fraction for the BNV mode is performed. The region $M_{bc} \leq 5.26 \text{ GeV}/c^2$ defines the sideband.

After applying all selection criteria, the percentages of reconstructed signal MC events that contain more than one candidate are, depending on the decay channel, between 6% and 17%. The candidate with the smallest cumulative χ^2 obtained from the kinematic fits to Ξ_c^0 , $\bar{\Lambda}_c^-$ and Ξ^- (when present in the decay chain) is selected as the best candidate. Depending on the channel, the best candidate is correctly reconstructed in between 72% and 94% of signal MC events with more than one candidate. The signal candidate is correctly reconstructed in between 85% and 97% of events with at least one candidate. Overall reconstruction efficiencies for individual channels are in the range between 6.6% and 9.9%. The average ratio of overall efficiencies for the BNV and SM modes using correctly-reconstructed signal events is 0.993 ± 0.004 , where the uncertainty is due to the limited size of our signal MC sample. Note that the effect of detection efficiency asymmetry between particles and antiparticles cancels in the ratio of branching fractions

for the BNV and SM modes, because charge conjugate final states are combined when estimating efficiencies and performing fits to data.

We measure branching fractions $\mathcal{B}(B^- \rightarrow \Xi_c^0 \bar{\Lambda}_c^-)$ and $\mathcal{B}(B^- \rightarrow \Xi_c^0 \bar{\Lambda}_c^-)$ for the SM and BNV modes. For each of the two measurements, a 2D unbinned extended maximum likelihood fit is performed simultaneously to M_{bc} vs ΔE distributions for the SM (BNV) decay $B^- \rightarrow \Xi_c^0 (\Xi_c^0) \bar{\Lambda}_c^-$ in the $\Xi_c^0 \rightarrow \Xi^- \pi^+$, $\Lambda^0 K^- \pi^+$ and $p K^- K^- \pi^+$ channels, summed over the two reconstructed $\bar{\Lambda}_c^-$ decay modes. Branching fractions of Ξ_c^0 and reconstruction efficiencies for individual channels are used to fix the relative yields in the fit. To handle signal correlations between M_{bc} and ΔE , a 2D smoothed histogram [29] obtained from signal MC samples is used to model the signal probability density function (PDF). Bin widths used for these histograms are 2 MeV/ c^2 and 2.5 MeV for M_{bc} and ΔE , respectively. We use the second-order interpolation between the bins. The same signal PDFs are used for the SM and BNV modes. The 2D background PDF is assumed to be factorizable, i.e., $\mathcal{P}_{bkg}(M_{bc}, \Delta E) = \mathcal{P}_{bkg}(M_{bc}) \times \mathcal{P}_{bkg}(\Delta E)$ as the correlations between M_{bc} and ΔE for background are found to be negligible. The background M_{bc} distribution is modeled with an ARGUS function [30] and the background ΔE distribution is modeled with a first-order Chebychev polynomial. No peaking backgrounds have been identified using MC samples. Background PDF parameters are not constrained in the fits. The fit results for the branching fractions for SM and BNV modes are $\mathcal{B}(B^- \rightarrow \Xi_c^0 \bar{\Lambda}_c^-) = (1.13 \pm 0.12) \times 10^{-3}$ and $\mathcal{B}(B^- \rightarrow \Xi_c^0 \bar{\Lambda}_c^-) = (-7.78 \pm 2.70) \times 10^{-5}$, where only the statistical uncertainty is shown. According to toy MC experiments, the probability to obtain such or even more negative a result for the BNV mode is 25%. Fig. 1 shows the signal-region projections of the fit results to data onto the M_{bc} and ΔE distributions for SM and BNV analyses. The result for the SM mode is consistent with the previous measurement from Belle [19]. The fit results correspond to 46.6 ± 4.9 (-3.2 ± 1.1), 49.6 ± 5.3 (-3.4 ± 1.2) and 20.9 ± 2.2 (-1.5 ± 0.5) events in the SM (BNV) modes $\Xi^- \pi^+$ ($\Xi^+ \pi^-$), $\Lambda^0 K^- \pi^+$ ($\bar{\Lambda}^0 K^+ \pi^-$) and $p K^- K^- \pi^+$ ($\bar{p} K^+ K^+ \pi^-$), respectively, where only the statistical uncertainty is shown.

Since we use the same analysis procedure for SM and BNV decays, most of the systematic uncertainties, such as contributions from luminosity, PID selection, track reconstruction, K_S^0 and Λ^0 reconstruction, cancel in the ratio between branching fractions for the BNV and SM modes. The only significant contribution to systematic uncertainty is due to the PDF parameterization which is taken into account in the upper limit estimation procedure which is described later. The systematic uncertainties due to finite MC statistics and imperfect knowledge of the daughter particle branching fractions are 0.4% and 0.02%, respectively. The effect of these uncertainties on

the final result is negligible.

To estimate the upper limit using the frequentist approach [31], we construct the 90% C.L. belt for the ratio between the branching fractions for the BNV and SM modes. We perform 5000 pseudo-experiments for each assumed ratio and randomly sample the SM mode branching fraction based on its measured value and statistical uncertainty in each toy MC experiment. We use this procedure to estimate the number of signal events in each of the SM and BNV modes. The expected numbers of background events in SM and BNV modes are estimated using sideband data scaled using background MC. Events are generated according to the fit models described previously. Finally, to measure the ratio between branching fractions for the BNV and SM modes, we fit our model with PDFs, that are randomly varied to incorporate systematic uncertainties due to PDF parametrization. To take into account the difference between data and MC resolution functions, the width of each signal PDF is modified using a scale factor randomly sampled from a Gaussian distribution with $\mu = 1$ and $\sigma = 0.1$, in order to increase or decrease the width of the signal PDFs by 10%, on average. In order to include systematic uncertainties due to background PDF shapes, the background M_{bc} distribution is modeled with an ARGUS function with released threshold and the background ΔE distribution is modeled with a second-order Chebychev polynomial. For each ensemble of pseudo-experiments, the lower and upper ends of respective confidence intervals correspond to the values for which 5% of the fit results are below and above these values. Fig. 2 shows the 90% C.L. belt for the ratio of branching fractions for the BNV and SM modes after including both statistical and systematic uncertainties.

Based on the central value of -0.069 for the measured ratio between branching fractions for the SM and BNV modes, the upper limit on their ratio, $R = \mathcal{B}(B^- \rightarrow \Xi_c^0 \bar{\Lambda}_c^-) / \mathcal{B}(B^- \rightarrow \Xi_c^0 \bar{\Lambda}_c^-)$ is estimated to be $< 2.7\%$ at the 95% C.L.

An alternative interpretation of our results is provided assuming that no direct BNV decay of B^- takes place. In this case R is the time-integrated ratio between Ξ_c^0 event rates for the BNV and SM modes given by Eq. 2. Assuming no direct BNV in Ξ_c^0 decays allows us to use Eq. 3 to estimate the upper limit on the oscillation angular frequency to be $\omega < 0.76 \text{ ps}^{-1}$ at the 95% C.L., equivalent to $\tau_{\text{mix}} > 1.3 \text{ ps}$.

Assuming a zero result for the B^- branching fraction for the BNV mode, the sensitivity for the ratio between branching fractions for the BNV and SM modes is $R = 5.6\%$ at the 95% C.L. Under the hypothesis of $\Xi_c^0 - \Xi_c^0$ oscillations a zero result corresponds to a sensitivity $\omega = 1.10 \text{ ps}^{-1}$ at the 95% C.L. for the oscillation angular frequency (equivalent to $\tau_{\text{mix}} > 0.91 \text{ ps}$).

In summary, using the full data sample collected by the Belle experiment at the $\Upsilon(4S)$ resonance, we per-

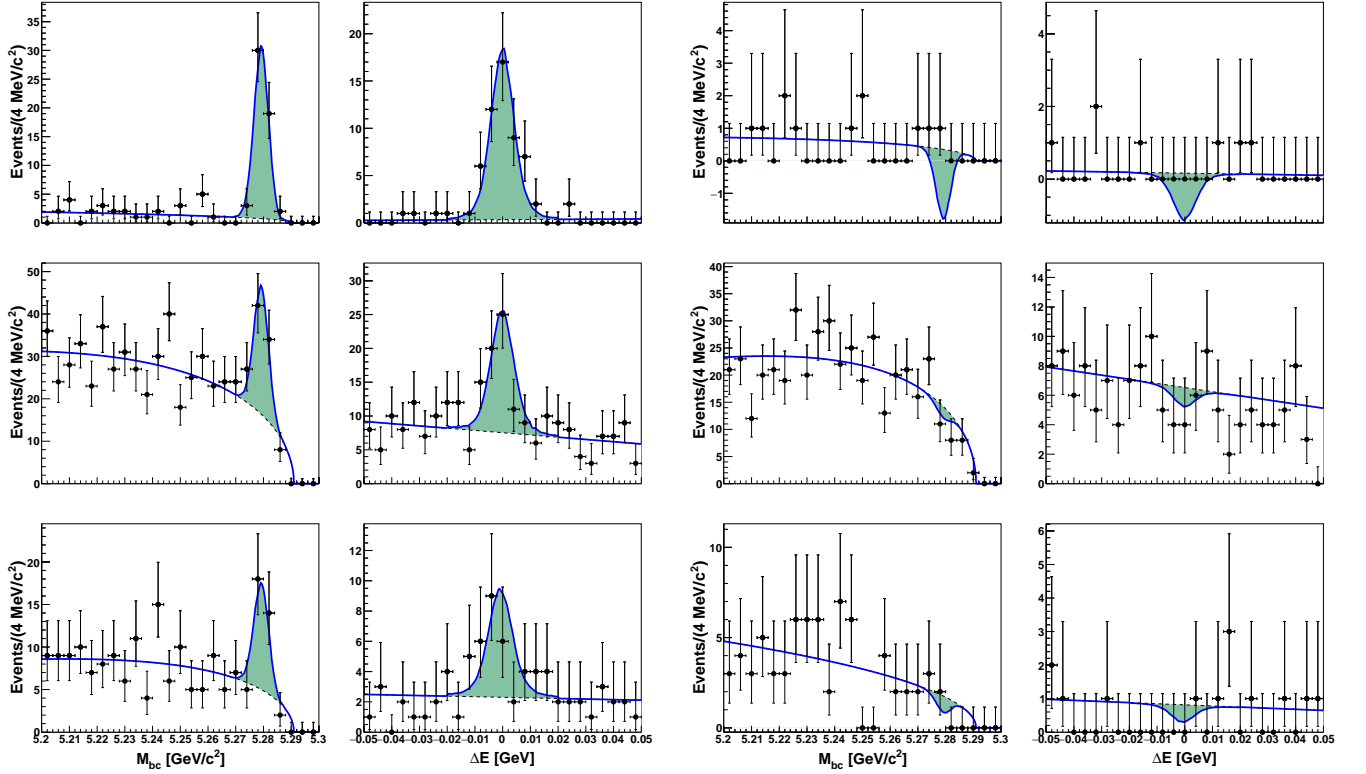


FIG. 1: Signal-region projections of the data fit result onto M_{bc} and ΔE for (left) the SM mode $B^- \rightarrow \Xi_c^0 \bar{\Lambda}_c^-$ and (right) the BNV mode $B^- \rightarrow \Xi_c^0 \bar{\Lambda}_c^-$ in the $\Xi_c^0 \rightarrow \Xi^- \pi^+$, $\Lambda^0 K^- \pi^+$ and $p K^- K^- \pi^+$ (top, middle and bottom) channels, summed over the two reconstructed $\bar{\Lambda}_c^-$ decay modes. Dots with error bars represent the binned data, blue solid curves show the results of the fit, green-filled regions and black dashed curves show the signal and background fit components, respectively.

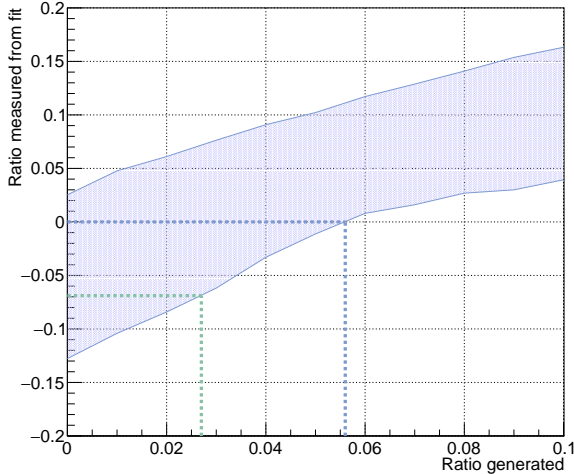


FIG. 2: The 90% C.L. belt for the ratio between branching fractions for the BNV and SM modes constructed including statistical and systematic uncertainties. Green and blue dotted lines demonstrate the procedures used to obtain our 95% C.L. upper limit and the sensitivity (using a zero result), respectively.

formed the first search for the baryon-number-violating processes in B^- decays to the $\Xi_c^0 \bar{\Lambda}_c^-$ final state. We observe no evidence for baryon number violation and set the 95% C.L. upper limit on the ratio between branching fractions for the BNV and SM modes in B^- decays to be $< 2.7\%$. Assuming no direct BNV transitions in Ξ_c^0 decays, we set the 95% C.L. upper limit on the $\Xi_c^0 - \bar{\Xi}_c^0$ oscillation angular frequency to be $< 0.76 \text{ ps}^{-1}$ (equivalent to $\tau_{\text{mix}} > 1.3 \text{ ps}$). This is the first experimental result on oscillations in the charmed baryon sector.

This work, based on data collected using the Belle detector, which was operated until June 2010, was supported by the Ministry of Education, Culture, Sports, Science, and Technology (MEXT) of Japan, the Japan Society for the Promotion of Science (JSPS), and the Tau-Lepton Physics Research Center of Nagoya University; the Australian Research Council including grants DP210101900, DP210102831, DE220100462, LE210100098, LE230100085; Austrian Federal Ministry of Education, Science and Research (FWF) and FWF Austrian Science Fund No. P 31361-N36; National Key R&D Program of China under Contract No. 2022YFA1601903, National Natural Science Foundation of China and research grants No. 11575017, No. 11761141009, No. 11705209, No. 11975076,

No. 12135005, No. 12150004, No. 12161141008, and No. 12175041, and Shandong Provincial Natural Science Foundation Project ZR2022JQ02; the Czech Science Foundation Grant No. 22-18469S; Horizon 2020 ERC Advanced Grant No. 884719 and ERC Starting Grant No. 947006 “InterLeptons” (European Union); the Carl Zeiss Foundation, the Deutsche Forschungsgemeinschaft, the Excellence Cluster Universe, and the VolkswagenStiftung; the Department of Atomic Energy (Project Identification No. RTI 4002), the Department of Science and Technology of India, and the UPES (India) SEED finding programs Nos. UPES/R&D-SEED-INFRA/17052023/01 and UPES/R&D-SOE/20062022/06; the Istituto Nazionale di Fisica Nucleare of Italy; National Research Foundation (NRF) of Korea Grant Nos. 2016R1D1A1B02012900, 2018R1A2B3003643, 2018R1A6A1A06024970, RS2022-00197659, 2019R1I1A3A01058933, 2021R1A6A1A-03043957, 2021R1F1A1060423, 2021R1F1A1064008, 2022R1A2C1003993; Radiation Science Research Institute, Foreign Large-size Research Facility Application Supporting project, the Global Science Experimental Data Hub Center of the Korea Institute of Science and Technology Information and KREONET/GLORIAD; the Polish Ministry of Science and Higher Education and the National Science Center; the Ministry of Science and Higher Education of the Russian Federation, Agreement 14.W03.31.0026, and the HSE University Basic Research Program, Moscow; University of Tabuk research grants S-1440-0321, S-0256-1438, and S-0280-1439 (Saudi Arabia); the Slovenian Research Agency Grant Nos. J1-9124 and P1-0135; Ikerbasque, Basque Foundation for Science, and the State Agency for Research of the Spanish Ministry of Science and Innovation through Grant No. PID2022-136510NB-C33 (Spain); the Swiss National Science Foundation; the Ministry of Education and the National Science and Technology Council of Taiwan; and the United States Department of Energy and the National Science Foundation. These acknowledgements are not to be interpreted as an endorsement of any statement made by any of our institutes, funding agencies, governments, or their representatives. We thank the KEKB group for the excellent operation of the accelerator; the KEK cryogenics group for the efficient operation of the solenoid; and the KEK computer group and the Pacific Northwest National Laboratory (PNNL) Environmental Molecular Sciences Laboratory (EMSL) computing group for strong computing support; and the National Institute of Informatics, and Science Information NETwork 6 (SINET6) for valuable network support. We thank David McKeen (TRIUMF) and Brian Batell (University of Pittsburgh) for stimulating discussions.

-
- [1] A. D. Sakharov, Violation of CP invariance, C asymmetry, and baryon asymmetry of the universe, *Sov. Phys. Usp.* **34**, 392 (1991).
 - [2] R. M. Bionta *et al.*, The search for proton decay, *AIP Conf. Proc.* **123**, 321 (1984).
 - [3] R. Godang *et al.* (CLEO Collaboration), Search for baryon and lepton number violating decays of the tau lepton, *Phys. Rev. D* **59**, 091303 (1999).
 - [4] D. Sahoo *et al.* (Belle Collaboration), Search for lepton-number- and baryon-number-violating tau decays at Belle, *Phys. Rev. D* **102**, 111101 (2020).
 - [5] P. del Amo Sanchez *et al.* (BABAR Collaboration), Searches for the baryon- and lepton-number violating decays $B^0 \rightarrow \Lambda_c^+ \ell^-$, $B^- \rightarrow \Lambda \ell^-$, and $B^- \rightarrow \bar{\Lambda}^0 \ell^-$, *Phys. Rev. D* **83**, 091101 (2011).
 - [6] W. S. Hou, M. Nagashima and A. Soddu, Baryon number violation involving higher generations, *Phys. Rev. D* **72**, 095001 (2005).
 - [7] V. A. Kuzmin, V. A. Rubakov and M. E. Shaposhnikov, On the Anomalous Electroweak Baryon Number Non-conservation in the Early Universe, *Phys. Lett. B* **155**, 36 (1985).
 - [8] P. Minkowski, On the Spontaneous Origin of Newton’s Constant, *Phys. Lett. B* **71**, 419 (1977).
 - [9] R. N. Mohapatra and G. Senjanovic, Neutrino Masses and Mixings in Gauge Models with Spontaneous Parity Violation, *Phys. Rev. D* **23**, 165 (1981).
 - [10] T. Han, H. E. Logan, B. Mukhopadhyaya and R. Srikanth, Neutrino masses and lepton-number violation in the littlest Higgs scenario, *Phys. Rev. D* **72**, 053007 (2005).
 - [11] D. G. Phillips II *et al.*, Neutron-antineutron oscillations: theoretical status and experimental prospects, *Phys. Rept.* **612**, 1 (2016).
 - [12] M. Ablikim *et al.* (BES III Collaboration), Search for $\bar{\Lambda} - \Lambda$ baryon-number-violating oscillations in the decay $J/\psi \rightarrow p K^- \Lambda + c.c.$, *Phys. Rev. Lett.* **131**, 121801 (2023).
 - [13] R. Aaij *et al.* (LHCb Collaboration), Search for baryon-number violating Ξ_b^0 oscillations, *Phys. Rev. Lett.* **119**, 181807 (2017).
 - [14] K. Aitken, D. McKeen, T. Neder and A. E. Nelson, Baryogenesis from oscillations of charmed or beautiful baryons, *Phys. Rev. D* **96**, 075009 (2017).
 - [15] H. E. Haber and G. L. Kane, The Search for Supersymmetry: Probing Physics Beyond the Standard Model, *Phys. Rep.* **117**, 75 (1985).
 - [16] R. L. Workman *et al.* (Particle Data Group), Review of particle physics, *PTEP* **2022**, 083C01 (2022).
 - [17] A. Abashian *et al.* (Belle Collaboration), The Belle detector, *Nucl. Instrum. Meth. A* **479**, 117 (2002).
 - [18] J. Brodzicka *et al.* (for the Belle Collaboration), Physics achievements from the Belle experiment, *PTEP* **2012**, 04D001 (2012).
 - [19] Y. B. Li *et al.* (Belle Collaboration), First measurements of absolute branching fractions of the Ξ_c^0 baryon at Belle, *Phys. Rev. Lett.* **122**, 082001 (2019).
 - [20] A. Lenz and G. Wilkinson, Mixing and CP Violation in the Charm System, *Ann. Rev. Nucl. Part. Sci.* **71**, 59 (2021).
 - [21] S. Kurokawa and E. Kikutani, Overview of the KEKB

- accelerators, Nucl. Instrum. Meth. A **499**, 1 (2003), and other papers included in this Volume; T. Abe *et al.*, Achievements of KEKB, PTEP **2013**, 03A001 (2013), and references therein.
- [22] D. J. Lange, The EVTGEN particle decay simulation package, Nucl. Instrum. Meth. A **462**, 152 (2001).
 - [23] E. Barberio and Z. Was, PHOTOS: A Universal Monte Carlo for QED radiative corrections. Version 2.0, Comput. Phys. Commun. **79**, 291 (1994).
 - [24] T. Sjostrand, S. Mrenna and P. Z. Skands, A Brief Introduction to PYTHIA 8.1, Comput. Phys. Commun. **178**, 852 (2008).
 - [25] R. Brun *et al.*, GEANT Detector Description and Simulation Tool, CERN ebook 10.17181/CERN.MUHF.DMJ1, (1994).
 - [26] E. Nakano, Belle PID, Nucl. Instrum. Meth. A **494**, 402 (2002).
 - [27] M. Feindt and U. Kerzel, The NeuroBayes neural network package, Nucl. Instrum. Meth. A **559**, 190 (2006).
 - [28] H. Nakano *et al.* (Belle Collaboration), Measurement of time-dependent CP asymmetries in $B^0 \rightarrow K_S^0 \eta \gamma$ decays, Phys. Rev. D **97**, 092003 (2018).
 - [29] W. Verkerke and D. P. Kirkby, The RooFit toolkit for data modeling, eConf **C0303241**, MOLT007 (2003).
 - [30] H. Albrecht *et al.* (ARGUS Collaboration), Search for hadronic $b \rightarrow u$ decays, Phys. Lett. B **241**, 278 (1990).
 - [31] J. Neyman, Outline of a theory of statistical estimation based on the classical theory of probability, Phil. Trans. Roy. Soc. Lond. A **236**, 333 (1937).